

Experimental study on chaos generation in an all-fiber erbium-doped fiber ring laser with a Mach-Zehnder interferometer

Mingxiang Ma (马明祥), Zhengliang Hu (胡正良)*, Pan Xu (徐攀), Wei Wang (王伟),
and Yongming Hu (胡永明)

College of Optoelectronic Science and Engineering, National University of Defense Technology,
Changsha 410073, China

*Corresponding author: zheng-liang-hu@163.com

Received March 28, 2014; accepted April 23, 2014; posted online July 18, 2014

We experimentally study the chaotic behaviors in a compact all-fiber erbium-doped fiber ring laser (EDFRL) with an added Mach-Zehnder interferometer (MZI) by using a phase-modulation method. A piezoelectric ceramic transducer (PZT) is incorporated in the MZI to introduce single-frequency phase modulation. The coexistence of intermittency and period-doubling bifurcation routes to chaos in the EDFRL system is observed by adjusting the modulation frequency or the phase modulation depth in the experiment. In addition, the EDFRL presents irregular multi-longitudinal-mode oscillation with a definite linear polarization when operating at intensity chaos state.

OCIS codes: 140.1540, 140.3510, 140.3500, 120.5060.

doi: 10.3788/COL201412.081403.

Chaos is an important branch of nonlinear science, and it occurs in many nonlinear systems, such as climate, finance system, species group, lasers, and so on. Erbium-doped fiber ring lasers (EDFRLs) have been widely investigated for their applications in communications, sensing, spectroscopy, and medicine^[1–8]. Meanwhile, these lasers are quite susceptible to any external perturbation that may destabilize their normal operation. Since the polarization variable can be adiabatically eliminated, EDFRLs belong to class-B lasers. Generally, when an additional degree of freedom is added in the form of either pump modulation^[9,10], loss modulation^[11,12], the nonlinear optical loop mirror (NOLM)^[13], or delay feedback^[14,15], chaos via period-doubling bifurcation, intermittency, and quasi-periodic routes can be observed in EDFRLs. In a loss-modulated EDFRL an electric optic modulator (EOM) or acoustic optic modulator (AOM) is usually employed as the loss modulator inserted in the laser cavity for chaos generation. To the NOLM scheme, the polarization controllers incorporated in the NOLM need to be adjusted exactly and fixed at an appropriate orientation. As for the delay-feedback scheme, numerical results indicate that generating chaos in simulation appears easier than in practical operation, because a piece of over-long delay fiber is required and the delay adjusting is not that convenient. However, the insertion of either EOM, AOM, NOLM, or an piece of over-long delay fiber in the EDFRLs will inevitably increase the complexity and the bulk of the cavity configuration, which may decrease the reliability of the laser system.

In this letter, we experimentally investigate the generation of chaos in a compact all-fiber EDFRL with an added Mach-Zehnder interferometer (MZI) by applying a phase modulation on the cavity fiber. Experimental results show that the coexistence of intermittency and period-doubling bifurcation routes to intensity chaos in the EDFRL system can be realized by modifying the

modulation frequency or the phase modulation depth.

The experimental setup of the all-fiber EDFRL with a MZI is shown in Fig. 1. The MZI is composed of two 3-dB polarization-maintaining (PM) fiber couplers C1 and C2, and is inserted into a primary ring cavity. The arm length difference (ALD) of the MZI is ~ 2.6 m, and one of its arms is wound on a piezoelectric ceramic transducer (PZT, with a diameter of 20 mm) for ALD control. The primary ring cavity consists of a PM 980/1550-nm wavelength division multiplexer (WDM), a 3-m-long piece of PM erbium-doped fiber (EDF, with a peak absorption of 18 dB/m at 980 nm), and a three-port polarization-dependent optical circulator (CIR). A 980-nm laser diode (LD) provides pump power for the EDF through the WDM. A 56%-reflectivity fiber Bragg grating (FBG, center wavelength ~ 1538.4 nm, 3-dB bandwidth ~ 0.12 nm) spliced with the second port of the CIR is used to obtain optical feedback, wavelength selection, and lasing output simultaneously. Note that the CIR ensures unidirectional traveling-wave oscillation with a definite linear polarization in the ring cavity. An optical isolator (ISO) is connected to the output pigtail to avoid back scattering light. The EDFRL is packed compact and mounted in an isolation metal case, making the laser system less sensitive to ambient vibrations.

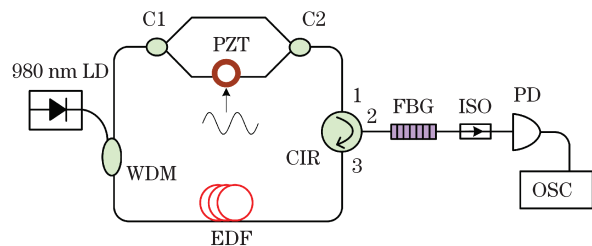


Fig. 1. (Color online) Experimental setup of the all-fiber EDFRL with a MZI.

Actually, the all-fiber EDFRL with a MZI in Fig. 1 can be treated as a compound-ring-cavity fiber laser and the PZT is just a phase modulator within the subcavity. The round-trip cavity lengths of the main cavity and the subcavity are approximately 9.2 and 11.8 m, respectively. We imposed a cosine phase modulation with a frequency f_0 and amplitude C on the MZI by applying a cosine voltage signal to the PZT. The output dynamics of the EDFRL was analyzed by measuring its intensity with a photodetector (PD) and a digital oscilloscope (OSC). As is known, if there exists a beam of single-frequency light propagating through the MZI, the interferential light intensity measured at the output of the MZI can be written as

$$I = A + B \cos[C \cos \omega_0 t + \varphi(t)], \quad (1)$$

where C is the phase modulation depth; ω_0 is the angular frequency that is equal to $2\pi f_0$; $\varphi(t)$ is the phase difference between the two arms of the MZI, i.e., the working point of the MZI; the constants A and B are both proportional to the input light intensity. Here, Eq. (1) can be expanded in terms of the Bessel functions^[16], expressed as

$$I = A + B \left\{ J_0(C) + 2 \sum_{k=1}^{\infty} (-1)^k J_{2k}(C) \cos 2k\omega_0 t \right\} \cos \varphi(t) - \left[2 \sum_{k=0}^{\infty} (-1)^k J_{2k+1}(C) \cos(2k+1)\omega_0 t \right] \sin \varphi(t). \quad (2)$$

Thus the MZI under phase modulation acts as an equivalent intensity modulator for each possible resonant mode oscillating in the fiber ring resonator.

Firstly, in our experiments the modulation frequency f_0 was used as the control parameter and the value of C was kept constant. Figure 2 shows the phase modulation efficiency of the PZT measured at different frequencies. The modulation efficiency curve exhibits uneven and tends to increase gradually from 0 to 40 kHz. To achieve the equivalent modulation depth for each frequency, as shown in Fig. 2, the amplitude of modulation voltage needs to be adjusted properly. In addition, the pump power was set as three times of the first threshold ($P_{th}=23$ mW), and the lasing output was measured to be about 3.2 mW. The EDFRL performs smooth and continuous-wave lasing output displayed by the OSC when no modulation signal is imposed on the MZI.

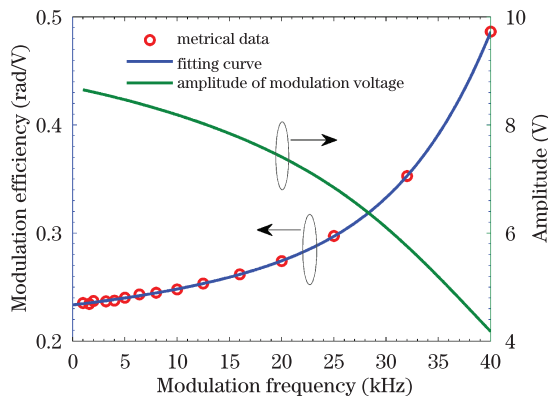


Fig. 2. (Color online) Modulation efficiency of the PZT and the amplitude of modulation voltage applied on the PZT with $C=2$ rad versus modulation frequency.

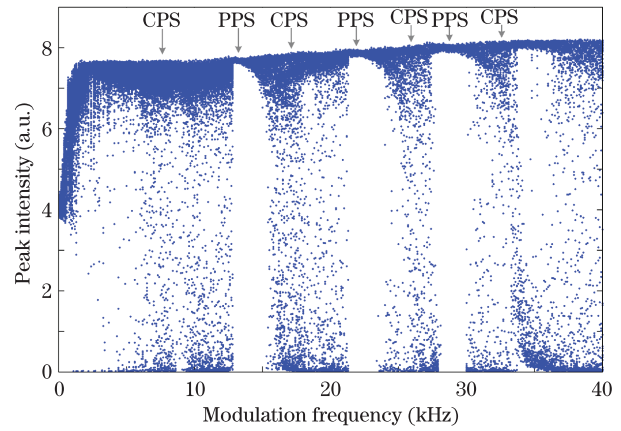


Fig. 3. (Color online) Bifurcation diagram of the output time series measured by sweeping the modulation frequency from 0.1 to 40 kHz. $C=2$ rad. $P=3P_{th}$.

The EDFRL exhibits various nonlinear dynamics in time domain under the phase modulation with different frequencies. Figure 3 illustrates the measured bifurcation diagram characterized by peak intensity distribution (PID) of the laser output time series, when the modulation frequency f_0 is swept gradually from 0.1 to 40 kHz and the value of C is set as 2 rad all along. Experimentally, we observe that the working mode of the EDFRL periodically switches between periodic pulse state (PPS) and chaotic pulse state (CPS) through a certain intermittency route (IR) as the modulation frequency is swept, as shown in Fig. 3. Thus the lasing chaotic states can be effectively controlled by adjusting the modulation frequency with C kept constant.

As an example, Fig. 4 describes one of the IR phenomena occurring within Fig. 3 in detail. It can be seen that the EDFRL temporarily operates at PPS from 12.8 to 13.7 kHz, which would be broken by intermittent chaos dynamics as the modulation frequency is further increased, and finally enters the CPS region ranging from 15.6 to 21.2 kHz.

Besides, there appears an intermittent chaos band in-laid among the CPS region from 32 to 40 kHz in Fig. 3, which indicates that the laser working mode may hop from one CPS to another through the IR with f_0 swept in high-frequency region. Then under low-frequency modulation the EDFRL output presents periodic relaxation-oscillation-like bursting dynamics. Note that a similar bifurcation diagram to Fig. 3 can be also measured by sweeping the modulation frequency with the value of C set as an optional value ranging from 0.5 rad to π rad in the experiment.

On the other hand, a period-doubling bifurcation route (PDBR) to chaos is also obtained experimentally, as shown in Fig. 5, when the phase modulation depth C is selected as the control parameter and the value of f_0 is kept constant instead. Figures 5(a)–(d) illustrate period-one, period-two, period-four, and chaotic states, respectively, where the value of C is set as 0.12, 0.24, 0.33, and 0.52 rad separately with $f_0=23$ kHz. The traces of these phase portraits in Figs. 5(a3)–(c3) appear slightly thickened, which is probably due to the slow drift of working point of the MZI under phase modulation. Our experimental results indicate that the slow

drift of working point induces little influence on the chaos generation that can be realized readily via above routes. The EDFRL would switch to a stable PPS again when the value of C is further increased beyond a threshold. As shown in Fig. 3, the EDFRL operates at PPS at the frequency of 23 kHz with $C=2$ rad.

The optical spectrum of the EDFRL at above CPS is measured by an optical spectrum analyzer, as shown in Fig. 6(a). A scanning Fabry-Perot interferometer (SFPI, free spectrum range=1.5 GHz, finesse=200) is used to monitor the longitudinal-mode structure of the EDFRL. Although the optical spectrum appears a single peak centered at 1538.4 nm, there dwells large numbers of longitudinal modes oscillating in the laser cavity. When

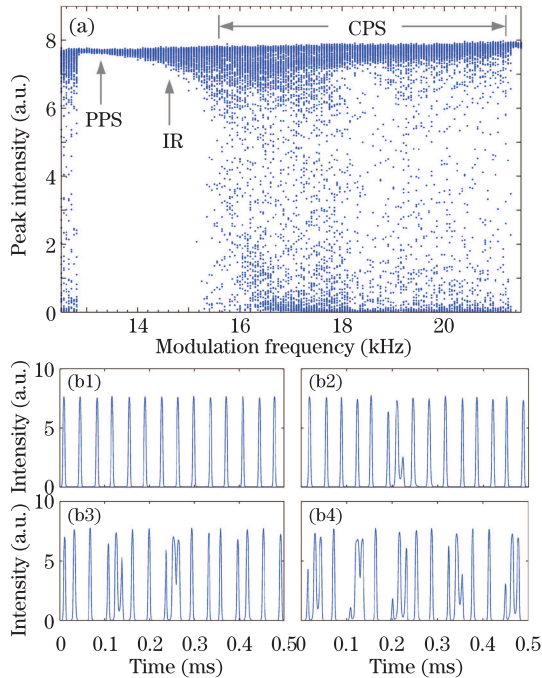


Fig. 4. (Color online) (a) Partial enlargement of Fig. 3 from 12.5 to 21.5 kHz. (b) Output time series with $C=2$ rad. The modulation frequencies are as follows: (b₁) 13.3 kHz, PPS; (b₂) 14.7 kHz, slight intermittency; (b₃) 15.3 kHz, intermittency; (b₄) 16.1 kHz, chaos.

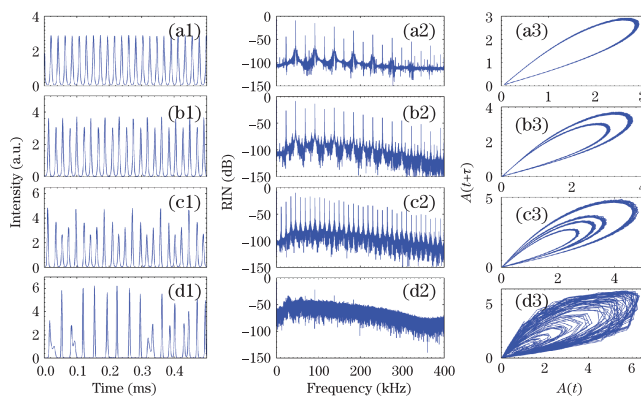


Fig. 5. (Color online) Time series, the corresponding relative intensity noise (RIN) spectra and phase portraits with $f_0=23$ kHz. The values of C are as follows: (a) $C=0.12$ rad, period-one; (b) $C=0.24$ rad, period-two; (c) $C=0.33$ rad, period-four; (d) $C=0.52$ rad, chaos.

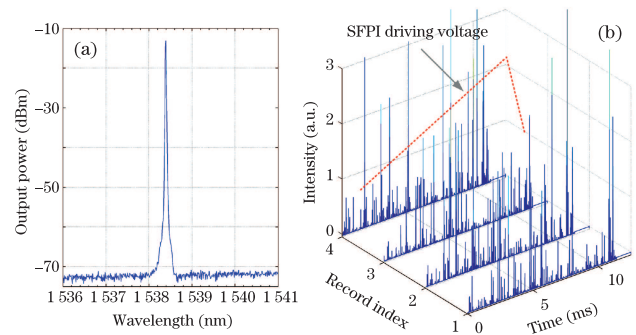


Fig. 6. (a) Measured output spectrum and (b) corresponding longitudinal-mode structure of the EDFRL operating at CPS.

operating at intensity chaos state in time domain, as shown in Fig. 6(b), the EDFRL exhibits irregular multi-longitudinal-mode (MLM) oscillation in frequency domain and each mode fluctuates stochastically in intensity due to drastic mode competition. The frequency dynamics^[17,18] of the EDFRL at intensity chaos state proves to be an open question, which should be related to high dimensional chaos because the optical intensity of each mode in Fig. 6(b) can be regarded as a single variable. Further investigations on the frequency dynamics are of great significance not only for their potential technological application, but also for fundamental research in nonlinear dynamics, and this will be the focus of our next work.

Moreover, the output dynamics is at a definite linear polarization state with a measured extinction ratio of ~ 29 dB, no matter whether the EDFRL operates at chaos state or not, because the CIR in PM fiber ring cavity can also act as a polarizer.

In conclusion, we report an experimental study on chaos generation in an all-fiber EDFRL with a MZI by using a phase-modulation method. A PZT is incorporated in the MZI to introduce single-frequency phase modulation. Experimental results indicate that the coexistence of IR and PDBR to intensity chaos in the EDFRL system is observed by adjusting the modulation frequency f_0 or the phase modulation depth C . The IRs to chaos are periodically obtained when f_0 is swept from 0.1 to 40 kHz with C set as 2 rad all along. Then the PDBR to chaos is also obtained when C varies from 0.12 to 0.52 rad with f_0 kept at 23 kHz. This phase-modulation method will be useful for applying chaos states in an all-fiber EDFRL, and make the configuration of chaotic fiber lasers relatively simple and compact. In addition, the EDFRL exhibits irregular MLM oscillation in frequency domain with a definite linear polarization when operating at intensity chaos state in time domain.

This work was supported by the National Natural Science Foundation of China under Grant No. 11274384.

References

1. D. Gregory, W. Van, and R. Rajarshi, *Science* **279**, 1198 (1998).
2. M. Dignonet, *Rare Earth-Doped Fiber Lasers and Amplifiers* (Marcel Dekker, New York, 1993).
3. M. A. Putnam, M. L. Dennis, I. N. Duling III, C. G. Askins, and E. J. Friebele, *Opt. Lett.* **23**, 138 (1998).

4. Y. Cheng, J. T. Kringlebotn, W. H. Loh, R. I. Laming, and D. N. Payne, *Opt. Lett.* **20**, 875 (1995).
5. K. Zhang and J. U. Kang, *Opt. Express* **16**, 14173 (2008).
6. X. Yang, L. Zhan, Q. Shen, and Y. Xia, *IEEE Photon. Technol. Lett.* **20**, 879 (2008).
7. H. Qi, J. Zhang, G. Zhou, A. Wang, and Z. Zhang, *Chin. Opt. Lett.* **11**, 061402 (2013).
8. S. J. Tan, S. W. Harun, H. Arof, and H. Ahmad, *Chin. Opt. Lett.* **11**, 073201 (2013).
9. L. G. Luo, T. J. Tee, and P. L. Chu, *J. Opt. Soc. Am. B* **15**, 972 (1998).
10. F. Zhang, P. L. Chu, R. Lai, and G. R. Chen, *IEEE Photon. Technol. Lett.* **17**, 549 (2005).
11. F. Chang, Y. Feng, Z. Yao, J. Fan, Y. Song, and Y. Zhao, *Chin. Phys. B* **21**, 100504 (2012).
12. Y. Liu, X. Feng, W. Zhang, and X. Liu, *Chin. Phys. B* **18**, 3318 (2009).
13. L. Yang, L. Zhang, R. Yang, L. Yang, B. Yue, and P. Yang, *Opt. Commun.* **285**, 143 (2012).
14. W. Fan, X. Tian, J. Chen, F. Zheng, Y. Yu, B. Gao, and H. Luo, *Chin. Phys.* **16**, 2908 (2007).
15. S. Zhang, H. Yang, and X. Qian, *Acta Phys. Sin.* **53**, 3706 (2004).
16. A. Dandridge, A. B. Tveten, and T. G. Giallorenzi, *IEEE J. Quantum Electron.* **18**, 1647 (1982).
17. D. Brunner, X. Porte, M. C. Soriano, and I. Fischer, *Sci. Rep.* **2**, 732 (2012).
18. D. J. DeShazer, J. García-Ojalvo, and R. Roy, *Phys. Rev. E* **67**, 036602 (2003).